Pergamon

Cement and Concrete Research 32 (2002) 289–296

CEMENT AND CONCRETE RESEARCH

Examining the relationship between the microstructure of calcium silicate hydrate and drying shrinkage of cement pastes

Maria C. Garci Juenger[a,1], Hamlin M. Jennings[a,b,*]

[a]*Department of Materials Science and Engineering, Northwestern University, Evanston, IL 60208, USA*
[b]*Department of Civil Engineering, Northwestern University, Evanston, IL 60208, USA*

Received 7 July 2000; accepted 23 August 2001

Abstract

Cement paste undergoes a volumetric contraction called drying shrinkage when placed in a low relative humidity (RH) environment. Only a portion of this shrinkage is reversible upon rewetting. In order to understand better the mechanisms responsible for the irreversible portion of drying shrinkage, a quantitative comparison was made between shrinkage values and microstructural properties of cement pastes. Drying shrinkage, surface area and pore volume were manipulated using curing temperature and chemical admixtures. It was observed that total and irreversible drying shrinkage increase with surface area and pore volume as measured by nitrogen (1–40 nm pore radius range), when degree of hydration and water-to-cement ratio (w/c) are held constant (0.55 and 0.45, respectively). © 2002 Elsevier Science Ltd. All rights reserved.

Keywords: Calcium–Silicate–Hydrate (C–S–H); Microstructure; Surface area; Shrinkage; Cement paste

1. Introduction

The volume of a hydrated cement paste or concrete specimen is sensitive to its moisture content, which can be controlled by the relative humidity (RH) of the surrounding environment. In less than 100% RH, a contraction is observed called drying shrinkage. If the same specimen is re-immersed in water, some of the volume is regained; this portion of the total drying shrinkage is thus called reversible or recoverable. Correspondingly, some of the deformation is permanent, called irreversible or irrecoverable shrinkage. The mechanisms responsible for reversible drying shrinkage are well developed, whereas those controlling irreversible drying shrinkage are still unclear.

Drying shrinkage is typically nonuniform throughout a sample and this leads to cracking and warping, which in turn cause durability problems including mechanical or esthetic failure, and pathways for the ingress of corrosive ions. As the RH cannot generally be controlled in real systems, it is of interest to control, instead, the response of the material to dry environments. In other words, shrinkage resistant concrete is desired.

The shrinking component in concrete is the cement paste. Several characteristics influence the degree of drying shrinkage, including the water-to-cement ratio (w/c) and age. Both of these affect the amount of capillary porosity, which is known to strongly affect drying shrinkage [1,2]. The age of a sample is also a reflection of how much of the main hydration product, calcium silicate hydrate (C–S–H), is present. C–S–H is highly porous, and thus will shrink upon drying. It is likely that drying shrinkage is affected not only by the quantity of C–S–H present, but by its microstructure as well.

One way of controlling drying shrinkage, therefore, may be by manipulating the microstructure of C–S–H. Cement paste composition, curing temperature and chemical and mineral admixtures are possible ways of changing the nature of C–S–H formed during hydration. To establish relationships between C–S–H microstructure and drying shrinkage, the effects of several variables on both must be compared. This requires quantitative measurements of both shrinkage and microstructure.

* Corresponding author. Tel.: +1-847-491-4858; fax: +1-847-491-5282.
E-mail address: h-jennings@northwestern.edu (H.M. Jennings).
[1] Present address: Department of Civil and Environmental Engineering; University of California, Berkeley; 721 Davis Hall; Berkeley, CA 94720, USA.

0008-8846/02/$ – see front matter
PII: S0008-8846(01)00673-1

Whereas there are standardized methods of measuring drying shrinkage, quantifying the microstructure of C–S–H is not trivial. Common observation techniques, such as microscopy, are primarily qualitative. Surface area techniques yield quantitative data, but the results are difficult to interpret. Sample preparation and data analysis are tricky, resulting in the dilemma that no two techniques for surface area measurement yield the same value for a given sample [3]. Several of the newer techniques, such as small angle X-ray and neutron scattering (SAXS and SANS), unfortunately require expensive equipment and intensive data analysis. Older techniques, such as water vapor and nitrogen adsorption, are quick and readily available and thus are ideal for collecting large data sets. Whereas surface area as measured by water vapor adsorption yields values that change little with variables such as w/c and composition, surface area as measured by nitrogen yields values that are more sensitive to variations in composition and processing [4]. In order to compare surface area and drying shrinkage, one must be able to vary both surface area and shrinkage by chemical manipulation of the system. Therefore, nitrogen adsorption was the method chosen for microstructural characterization in this work. Cement pastes were chosen instead of mortar or concrete for a similar reason; paste shrinks more than the others, and the ability to measure significant variation between samples is important.

There is evidence in the literature of relationships between surface area and shrinkage, beginning with the early theories of Powers and Brownyard [5]. Feldman and Swenson [6] showed rough correlations between increased nitrogen surface area and high total drying shrinkage for samples containing admixtures of calcium lignosulphonate, hydroxycarboxylic acid and triethanolamine. Bentur et al. [7–9] showed that the surface area of calcium silicate pastes decreased after being subjected to drying shrinkage and creep tests. They also reported a relationship between the extent of drying shrinkage for a given sample type and the surface area and porosity of parallel samples that were not subjected to shrinkage testing.

In the present study, a comparison is made between surface area, pore volume and drying shrinkage using the following variables: curing temperature (both higher and lower than room temperature), calcium chloride admixture and increased alkalinity. These are all variables that have been shown in previous studies to influence the surface area as measured by nitrogen [4,10]. All of the results presented are for samples with a degree of hydration of 0.55, and are thus representative of relatively young pastes. The influence of aging, therefore, is not included in this study.

2. Methods

Cement pastes for hydration, surface area, and porosity studies were made from ASTM Type I Portland cement (Table 1) with a w/c of 0.45. Batches were small (10–200 g), and mixing was done by hand for 5 min with a stainless steel spatula. Samples were cast in polystyrene vials (25 mm diameter, 50 mm height) and sealed in air-tight containers in a 20 °C water bath for the first 24 h. The containers were then filled with lime-water, sealed and placed in the 20 °C bath for the duration of the curing period, 1–270 days.

Table 1
Properties of ASTM Type I Portland cement

Phase	Weight percent
SiO_2	20.79
Al_2O_3	5.31
FE_2O_3	2.25
CaO	63.54
MgO	3.72
SO_3	2.84
C_3S	54
C_2S	19
C_3A	10
C_4AF	7
Properties	
Loss of ignition	1.09
Insoluble residue	0.1
Free lime	–
Sodium equivalent of alkalis	0.51
Blaine fineness (m^2/kg)	368

Further samples were cured in a 2 °C refrigerator and a 40 °C water bath in order to observe the effects of curing temperature. Specimens containing calcium chloride were cured at 20 °C, and 1% $CaCl_2{\cdot}2H_2O$ by weight of cement was dissolved in the mixing water. Sodium hydroxide was added as a 1-M solution in place of the mixing water; these samples were also cured at 20 °C.

After the specified hydration time, samples were removed from the molds and ground to particle sizes in the range of 600 (#30 sieve) to 1180 μm (#16 sieve). These were then D-dried for 14 ± 1 days. The D-drying apparatus was set up according to the method of Copeland and Hayes [11], and consists of vacuum drying to the vapor pressure of water at the temperature of dry ice (5×10^{-4} Torr). Equilibrium D-drying time was measured to be approximately 14 days; samples were tested immediately after drying.

Particles smaller than 600 μm were used for loss on ignition testing in order to determine degree of hydration (α). Approximately 3 g of these particles were placed in a furnace at 105 °C for at least 24 h, weighed and heated to 1005 °C for 2 h, decomposing most of the hydration products. The samples were then returned to 105 °C and reweighed. The degree of hydration was calculated using the following equation:

$$\alpha = \frac{W_{105} - W_{1005}}{0.24 \times W_{1005}} \tag{2.1}$$

where W_{105} and W_{1005} are the sample weights before and after firing to 1005 °C, respectively [12].

Nitrogen adsorption and desorption were done using a Coulter Omnisorp 360 (Coulter Corporation, Hialeah, FL). Surface area was calculated using the Brunauer, Emmett and

Table 2
Experimental matrix for porosity and shrinkage studies ($\alpha = .55$)

Sample type	w/c	Curing temperature (°C)	Age (days)
Control	0.45	20	3
Low temperature	0.45	2	14
High temperature	0.45	40	1
1% $CaCl_2$	0.45	20	3
1 M NaOH	0.45	20	7

Teller (BET) method of analysis [13] over a relative pressure range of 0.05–0.25 on the adsorption isotherm. Porosity and pore size distribution were calculated by the Barrett, Joyner and Hallenda (BJH) method [14] using data from the desorption isotherm. This technique only measures pores in cement pastes with radii between 1 and 40 nm.

Drying shrinkage was measured following ASTM standard C-596 [15]; the standard for mortars was adapted for use with pastes as follows. Cement pastes of w/c = 0.45 were hand mixed in 1 kg (cement weight) batches for 5 min and cast into polycarbonate molds with bar sizes of $25 \times 25 \times 250$ mm. The molds were kept at 100% RH at the appropriate temperature (2, 20 or 40 °C) for the first 24 h. At this point, samples were removed from the molds and placed in lime-water (2, 20 or 40 °C) for the remainder of curing. The samples were cured until a degree of hydration of approximately 0.55 was achieved, which is equivalent to a 3-day-old control sample (Table 2). After curing, samples were placed in a 50% RH, 22 °C environmental chamber for 84 days and the length change was measured periodically. Very little hydration continues during the drying period as the rate of water loss is fast, effectively halting further hydration. Irreversible shrinkage was then determined by placing the samples in lime-water for 14 days. Five bars from two different mixing batches were measured for all samples.

3. Results

Varying curing temperature and cement chemistry necessarily changes the rate at which a paste hydrates as shown in Fig. 1 (each point shown is the mean of three or more values, standard deviations ≅0.02). As expected, lowering the curing temperature significantly retards hydration, whereas a higher curing temperature accelerates hydration [4]. The effects of temperature become negligible at later ages. Calcium chloride is a known accelerator, but its effects are most apparent in the first 2–4 h of hydration. In concentrations of 1% it has no effect on degree of hydration for cement pastes with ages greater than one day [4]. Although a 1-M solution of sodium hydroxide accelerates early hydration (< 1 day), it subsequently retards later hydration [10].

Because curing temperature and admixtures change the rate of paste hydration, it is important to examine properties such as surface area and shrinkage of samples with similar

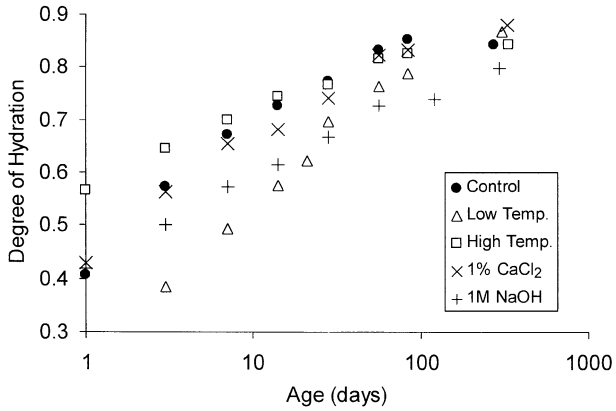

Fig. 1. Progression of hydration over time for cement pastes.

degrees of hydration rather than similar ages. The data in Fig. 2 (each point shown is the mean of three or more values, standard deviations ≅2.5) show that the surface areas available to nitrogen change with age and are strongly affected by the variables of interest. Compared to the room temperature control, high temperature curing (40 °C) has no effect, but low temperature curing (2 °C) increases surface area [4]. Calcium chloride increases surface area while sodium hydroxide decreases it [4,10].

The strongest effects of the variables on surface area are seen in the degree of hydration range of 0.45–0.75. In order to see the clearest relationship between surface area and shrinkage, differences should be maximized. Samples for further examination (drying shrinkage, porosity, etc.) were therefore chosen within this degree of hydration range.

Total drying shrinkage is also highly dependent on the age of the specimen before drying as shown in Fig. 3 for samples cured at 40 °C (each point shown is the mean of five values, standard deviations ≅0.007). It is clear that the younger the paste, the more it shrinks during drying at 50% RH. Sample age similarly affects the reversibility of shrinkage as shown in Fig. 3b (each point shown is the mean of five values, standard deviations ≅0.005). Because samples with high shrinkage should be studied, a degree of hydration

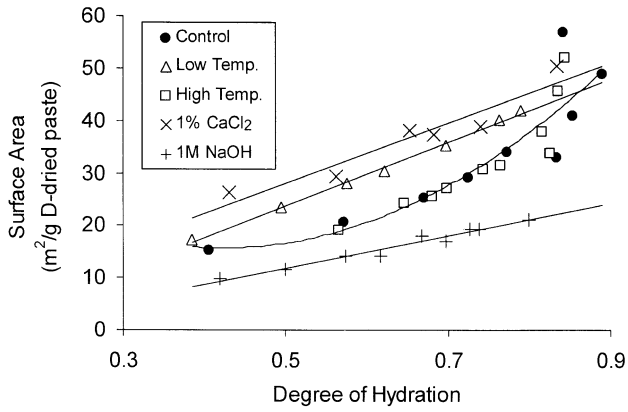

Fig. 2. Development of nitrogen surface area over time in cement pastes.

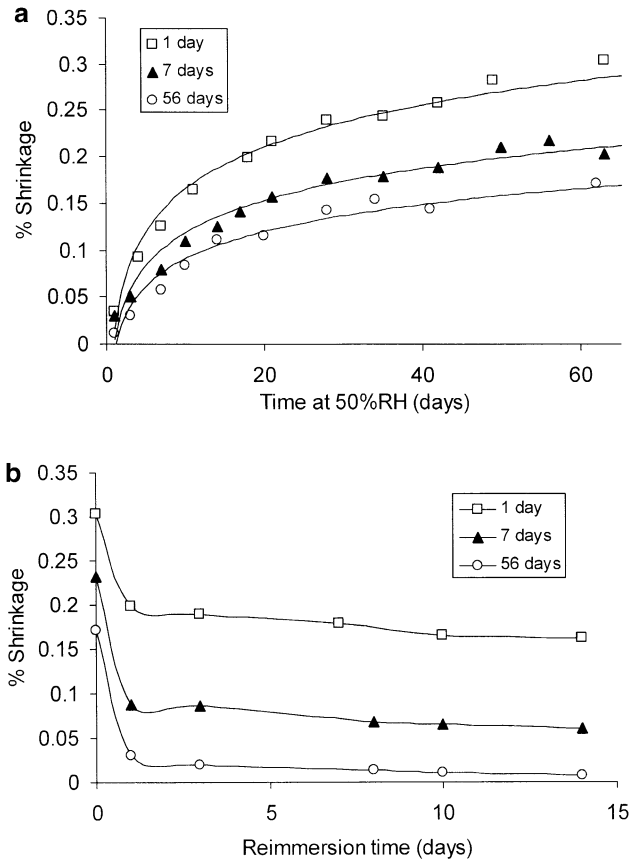

Fig. 3. Effect of age (time of moist curing at 40 °C) on: (a) total drying shrinkage at 50% RH, (b) irreversible drying shrinkage (immersed in lime-water after drying).

of 0.55, equivalent to the 1-day-old sample in Fig. 3a and b, was chosen as the standard for further studies (Table 2).

The surface area of cement paste as measured by nitrogen is dominated by the porosity of the C–S–H phase in the pore radius range of 1–40 nm. This porosity can be broken down into various pore size components as shown in Fig. 4 (data are from single samples but are representative of several tests). Results are necessarily similar to the surface area trends, as they are reflections of the same features. Pore size distribution is useful in that it can be used to pinpoint

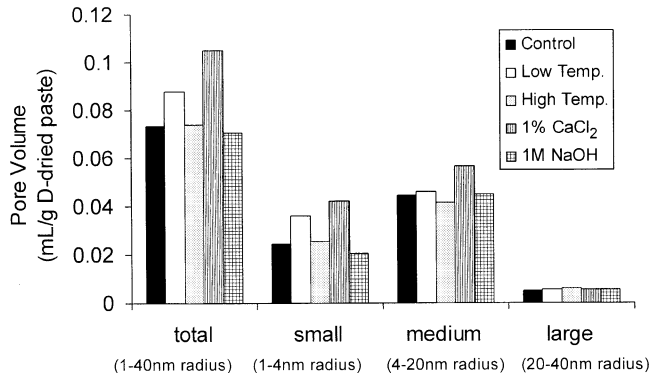

Fig. 4. Total pore volume available to nitrogen and pore size distribution in cement pastes of $\alpha \cong .55$.

which size range of C–S–H porosity has the strongest relationship to drying shrinkage.

Total drying shrinkage results for samples of $\alpha \cong 0.55$ are shown in Fig. 5a (each point shown is the mean of five values, standard deviations $\cong 0.02$). The rate of weight loss during drying is shown in Fig. 5b (no data are available for the high temperature samples). That the weight loss does not vary between samples is a reasonable result since the volume of capillary porosity is held constant. It is important to note that this drying shrinkage study was done at a single RH (50%) as dictated by the ASTM standard [15], rather than by equilibrating at successively lower relative humid-

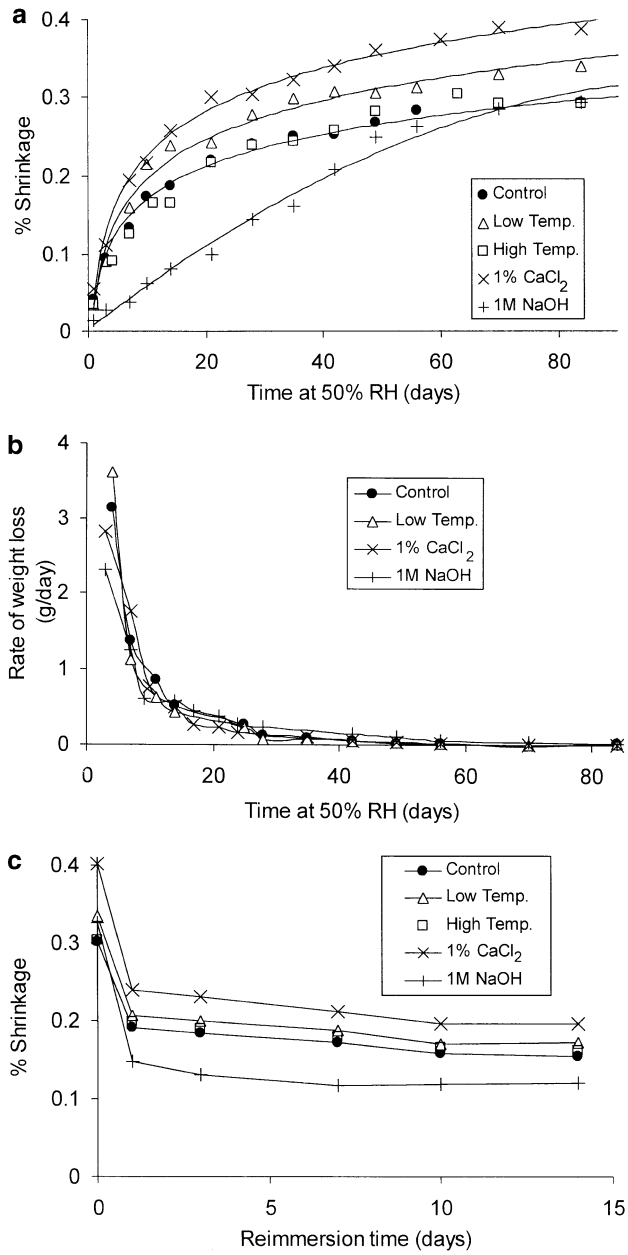

Fig. 5. Drying shrinkage data for cement pastes of $\alpha \cong .55$, dried at 50% RH: (a) total drying shrinkage, (b) rate of water loss during drying (c) irreversible drying shrinkage (immersed in lime-water after drying).

Table 3
Drying shrinkage results

	Percent change in length				
Type of drying shrinkage	Control, 20 °C	2 °C curing	40 °C curing	1% $CaCl_2$	1 M NaOH
Total	0.294 ± 0.026	0.340 ± 0.010	0.292 ± 0.006	0.389 ± 0.028	0.326 ± 0.006
Irreversible	0.155 ± 0.006	0.172 ± 0.008	0.162 ± 0.009	0.196 ± 0.011	0.121 ± 0.005
Reversible	0.139 ± 0.026	0.168 ± 0.010	0.130 ± 0.009	0.193 ± 0.028	0.205 ± 0.006

ities. This method gives us little information on the dynamics of shrinkage and weight loss, but does give us a valuable equilibrium value of drying shrinkage at 50% RH.

Results from the re-immersion of samples after drying are shown in Fig. 5c (each point shown is the mean of five values, standard deviations ≅0.009). In Fig. 5c, a time of 0 days is equivalent to the final time in Fig. 5a. Results are summarized in Table 3, where total drying shrinkage is the equilibrium value in Fig. 5a, irreversible drying shrinkage is the equilibrium value in Fig. 5c, and reversible shrinkage is the difference between the two. Curing at a higher than normal temperature (40 °C) has no effect on any type of drying shrinkage at 50% RH for w/c = 0.45, $\alpha = 0.55$. Low temperature curing (2 °C) increases total and irreversible drying shrinkage, but has no effect on reversible shrinkage. Calcium chloride causes higher shrinkage of all types. Sodium hydroxide retards the rate of drying shrinkage, but the total value is the equivalent to the control [10]. It increases reversible drying shrinkage, and decreases the irreversible component.

4. Discussion

It has often been reported in the literature that high curing temperatures decrease drying shrinkage [9,16–20]. Bentur et al. [9] showed that increasing the temperature (65 °C) decreased both reversible and irreversible shrinkage. Bentur [16] observed differences in the pore size distributions of samples cured at different temperatures but concluded that there was no simple correlation between pore size and amount of shrinkage. An increase in the size of the mesopores (1.5–15 nm radius range, as measured by mercury intrusion, nitrogen and water vapor adsorption) was related to increased shrinkage, but he suggested that the effects were more complicated. In the present study, high temperature curing had no effect on drying shrinkage. Perhaps, 40 °C is not hot enough to cause significant differences in the structure of C–S–H.

Curing at lower than room temperature has been shown to have the opposite effect on shrinkage as high temperature curing. Bentur [16] showed that for well hydrated samples of w/c = 0.4, those cured at 4 °C exhibited four times the drying shrinkage of those cured at 25 °C. In the present study, low temperature curing increased shrinkage, but not as dramatically as that reported by Bentur [16].

The increase in total drying shrinkage caused by calcium chloride is well documented [21–25]. Bentur et al. [21] also observed that $CaCl_2$ increased both the reversible and irreversible shrinkage. They attributed this to an increase in mesoporosity.

In a review on the effects of alkalis on cement pastes, Jawed and Skalny [26] concluded that shrinkage increased with increasing amount of alkali. Pickett [27] showed slightly higher shrinkage values for samples with 1% NaOH addition, but the rate of shrinkage was slower, which agrees with the results presented in this paper. He also showed that cements with a high alkali content have higher shrinkage stresses and greater cracking. The difference in rate of length change on drying for samples containing NaOH may be due to differences in cracking as discussed in Ref. [10].

4.1. Relationships between surface area, porosity and drying shrinkage

The total, equilibrium drying shrinkage as well as the irreversible and reversible components were plotted against surface area and pore volumes in all ranges across all variables. A least-squares line was fit to each plot, and the results are summarized in Table 4. All slopes are positive, indicating that all types of drying shrinkage increase with increasing C–S–H surface area and pore

Table 4
Correlation of drying shrinkage with surface area and pore volume

Drying shrinkage type	Surface area	Total pore volume (1–40 nm radius)	Small pores (1–4 nm radius)	Medium pores (4–20 nm radius)	Large pores (20–40 nm radius)
Total: slope	0.0046	2.593	4.0992	6.4703	27.881
R^2	.4303	.7629	.7235	.7232	.1721
Irreversible: slope	0.0035	1.677	2.8287	3.7514	17.272
R^2	.6526	.8292	.8953	.6318	.1717
Reversible: slope	0.0011	0.916	1.2705	2.7189	10.609
R^2	.0596	.2365	.1258	.3172	.0619

volumes. More in-depth statistical analysis cannot be done with this data because the pore volume and surface area data are so highly correlated. In other words, increases in surface area are generally accompanied by increases in pore volumes of all sizes. Furthermore, increases in pore volume of one size range are generally accompanied by increases in pore volume in the other size ranges. Therefore, the effects of surface area and pore volumes on shrinkage are not independent and cannot be separated. The least-squares plots summarized in Table 4 only have the power to tell us whether correlations are positive or negative, and which relationships are the strongest (i.e., those with the highest R^2 values).

Several of the relationships shown in Table 4 are very weak, as seen by the low R^2 values, particularly those for reversible shrinkage. The facets of C–S–H microstructure that are manipulated by temperature and admixtures must have only minimal effects on reversible shrinkage. Reversible shrinkage may be more dependent on the relatively large pores that are emptied of water at 50% RH than on the relatively small pores that are measured by nitrogen. It is also known that reversible shrinkage is dependent on the mass of C–S–H present, as determined by the degree of hydration for a given w/c (Fig. 3a and b), and the volume of capillary porosity for a given degree of hydration (w/c). Both the mass of C–S–H (α) and the w/c were kept constant in this study, confirming that there should be little correlation between reversible shrinkage and surface area/porosity as measured by nitrogen.

Plots for the strongest relationships between pore volumes and total and irreversible shrinkage are shown in Fig. 6a and b. Total drying shrinkage correlates best with total pore volume measurable by nitrogen (1–40 nm radius). Irreversible drying shrinkage correlates best with small pore volume (1–4 nm radius). In fact, the correlation coefficient for the latter is quite high, suggesting a very strong relationship.

4.2. Small pore volume and irreversible drying shrinkage

The samples in this study showed strong correlations between high total and irreversible drying shrinkage and high surface area and pore volume. Since reversible shrinkage was independent of surface area (Table 4), the increase in total shrinkage with surface area is only a reflection of the increase in the irreversible portion. It is appropriate, therefore, to focus only on the root of the differences, irreversible shrinkage.

The relationship between small pore volume as measured by nitrogen and irreversible drying shrinkage is so strong as to suggest the presence of an underlying physical mechanism. While one cannot justly say that strong correlations signify cause and effect, there must be some explanation for the relationship. A probable mechanism based on the data presented in this paper is outlined below. One must keep in mind that there are likely several mechanisms operating simultaneously to cause both reversible and irreversible shrinkage, and this is just one of the possibilities.

The phases in cement paste can be subdivided into two categories for the purposes of understanding drying shrinkage: restraining phases and shrinking phases. Unhydrated cement particles and some reaction products such as calcium hydroxide and ettringite do not deform on drying and are thus called restraining phases. Small pores and C–S–H shrink on drying. The degree to which a cement paste shrinks depends largely on the proportions and distributions of these two types of phases. Shrinkage may also be dependent on the morphology of these phases.

It is well documented that there may be more than one type of C–S–H, which may form by different mechanisms. These types have been called by various names: inner and outer product [28]; Types I–IV [29]; early, middle and late products [30]; and phenograin and groundmass [31]. The definitions and boundaries of these types are different, but the concepts are essentially the same. The inner/phenograin

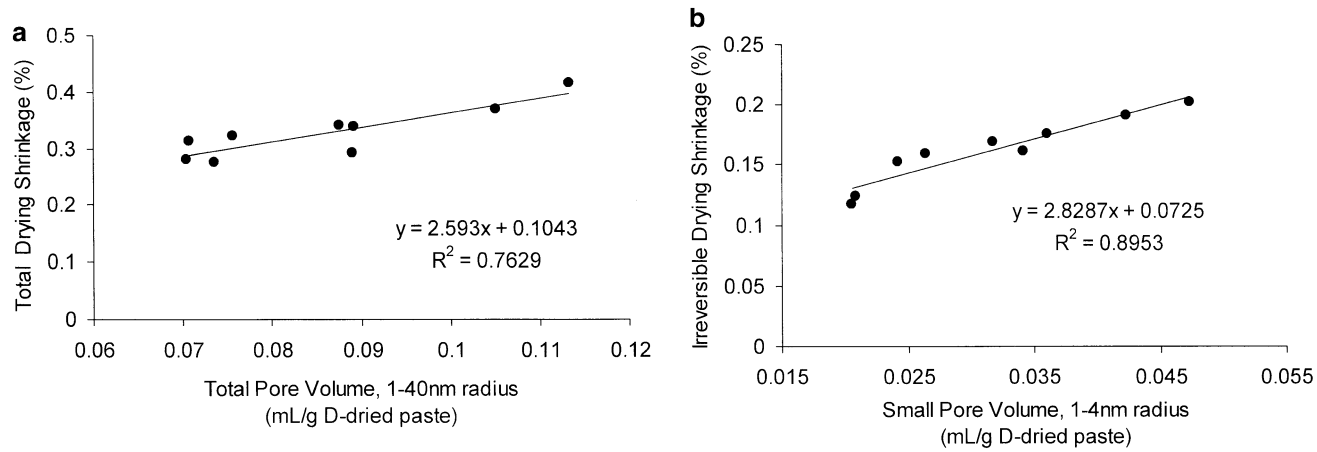

Fig. 6. (a) Relationship between total drying shrinkage and total pore volume available to nitrogen (1–40 nm radius) for cement pastes of $\alpha \cong .55$, (b) relationship between irreversible drying shrinkage and volume of small pores (1–4 nm radius) for cement pastes of $\alpha \cong .55$.

C–S–H appears characteristically denser in a SEM than the outer/groundmass. Jennings and Tennis [32,33] also discussed the possibility of two types of C–S–H based on nitrogen and water vapor adsorption data. One type of C–S–H is accessible to nitrogen while the other is accessible only to water vapor. This model did not contain a physical description of how one type of C–S–H inhibits nitrogen access. Combining these two concepts, Jennings and Tennis [34,35] proposed that the C–S–H which nitrogen cannot penetrate is denser, thus, containing smaller pores and possibly more "ink-bottle" pore entrances. The C–S–H that nitrogen can penetrate is less dense; the larger pores allow access to the nitrogen molecule. These two types of C–S–H they called high density (HD) and low density (LD).

Because HD is denser, it is probably much more resistant to drying shrinkage than LD. Furthermore, at 50% RH, the HD may still be saturated [34]. Perhaps, then, HD can be placed in the restraining phase category, while LD remains in the shrinking phase category. The ratio of LD to HD (LD/HD) in a cement paste would thus have a strong impact on drying shrinkage. For samples with the same degree of hydration and w/c, the total mass of C–S–H is constant, but the LD/HD may vary due to curing temperature and admixtures. Because HD and LD are defined in terms of their accessibility to nitrogen, surface area as measured by nitrogen (for a given α) is a reflection of this LD/HD. In other words, it can be said that for a given mass of C–S–H, the higher the surface area, the higher the LD/HD [36]. Table 4 thus shows conclusively that the higher the LD/HD, the higher the total and irreversible drying shrinkage. The reversible drying shrinkage is not affected much by this ratio because this type of shrinkage is more dependent on the relatively large pores that are emptied at 50% RH. The structure of these pores does not depend on the LD/HD ratio.

The samples in this study had constant capillary porosity and mass of C–S–H (equivalent w/c and degree of hydration); the only noticeable difference is in the morphology of the C–S–H. The differences in irreversible shrinkage may therefore be attributable to the different LD/HD. It can be concluded that the shrinkage of LD may be irreversible.

Fig. 7 shows a schematic diagram of what may happen to cement paste during drying at 50% RH. When capillary pores are emptied of water, a compressive stress is exerted on the pore walls, causing the solid material to contract. In cement pastes, the unhydrated cement and HD cannot deform during this contraction. Instead, the LD phase compacts, allowing the restraining phases to come closer together. Compaction of the LD phase occurs even though gel pores are not emptied by the drying process at 50% RH. This compaction is a process that may be similar to shrinkage that occurs in colloids known as the first falling rate period [34,37,38]. Upon rewetting, the volume of capillary pores is mostly recovered, while the volume of the LD phase is not completely recovered. The fact that irreversible shrinkage is most highly correlated with the volume of small

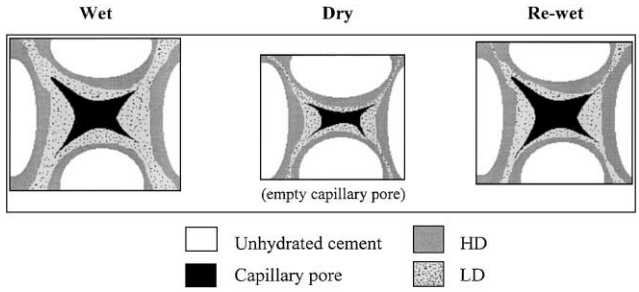

Fig. 7. Schematic diagram of cement paste shrinkage during drying at 50% RH: capillary pores and LD compact when dried, while HD and unhydrated cement (restraining phases) do not deform; on rewetting, capillary pores regain original shape, while LD does not.

pores (1–4 nm radius) suggests that the volume of small pores is related to the amount of collapsed LD.

Possible confirmation for this theory comes from the research of Bentur et al. [7,8]. They showed that in young pastes, the pore volume as measured by nitrogen in the radius range of 2–5 nm decreased after samples were dried at 53% RH. Furthermore, the nitrogen surface area (measured after drying at 53% RH) decreased with increasing irreversible shrinkage. These results agree with the concept that small pores within LD irreversibly collapse on drying, reducing surface area and pore volume in that region.

5. Conclusions

The nitrogen surface area and pore volume as well as drying shrinkage of cement paste can be manipulated using curing temperature regimes and chemical admixtures. In this investigation, comparisons were made at constant w/c and degree of hydration because these are known to strongly influence drying shrinkage and may have masked the subtler effects of curing temperature and chemical admixtures. It was observed that high surface areas and pore volumes corresponded with high values of total and irreversible drying shrinkage. Reversible drying shrinkage was independent of surface area and pore volume as measured by nitrogen.

There may be several parallel mechanisms at play influencing the rate and degree of drying shrinkage. The results of these experiments suggest that one mechanism may be dependent on the morphology of C–S–H, which can be chemically manipulated. C–S–H can be divided into two types, one with a higher density than the other (HD and LD), the former being inaccessible to nitrogen and perhaps nonshrinking. The LD portion of C–S–H may irreversibly shrink during drying at 50% RH.

Acknowledgments

The work presented in this paper was funded by the National Science Foundation Center for Advanced Cement

Based Materials and the Department of Energy (Grant #DE-FG02-91ER 45460-A003). MCGJ would like to thank N.S.F. for a Graduate Fellowship and G.E. for a Faculty for the Future Internship. Thanks also to A. Saak and D. Rossing for their help with the experiments described in this paper.

References

[1] R.A. Helmuth, D.H. Turk, The reversible and irreversible drying shrinkage of hardened Portland cement and tricalcium silicate pastes, J. Port. Cem. Assoc. Res. Dev. Lab. 9 (2) (1967) 8–21.
[2] G.J. Verbeck, R.A. Helmuth, Structures and physical properties of cement paste, Proceedings of the 5th International Congress on the Chemistry of Cement, vol. III, 1969, pp. 1–32.
[3] J.J. Thomas, H.M. Jennings, A.J. Allen, The surface area of hardened cement paste as measured by various techniques, Concr. Sci. Eng. 1 (1999) 45–64.
[4] M.C.G. Juenger, H.M. Jennings, The use of nitrogen adsorption to assess the microstructure of cement paste, Cem. Concr. Res. 31 (2001) 883–892.
[5] T.C. Powers, T.L. Brownyard, Studies of the physical properties of hardened Portland cement paste, Proc. Am. Concr. Inst. 43 (1946) 101.
[6] R.F. Feldman, E.G. Swenson, Volume change on first drying of hydrated Portland cement with and without admixtures, Cem. Concr. Res. 5 (1975) 25–35.
[7] A. Bentur, N.B. Milestone, J.F. Young, Creep and drying shrinkage of calcium silicate pastes: II. Induced microstructural and chemical changes, Cem. Concr. Res. 8 (1978) 721–732.
[8] A. Bentur, R.L. Berger, F.V. Lawrence, N.B. Milestone, S. Mindess, J.F. Young, Creep and drying shrinkage of calcium silicate pastes: III. A hypothesis of irreversible strains, Cem. Concr. Res. 9 (1979) 83–96.
[9] A. Bentur, J.H. Kung, R.L. Berger, J.F. Young, N.B. Milestone, S. Mindess, F.V. Lawrence, Influence of microstructure on creep and drying shrinkage of calcium silicate pastes, Proceedings of the 7th International Congress on the Chemistry of Cement, III (VI), 1980, pp. 26–31.
[10] M.C.G. Juenger, H.M. Jennings, Effects of high alkalinity on cement pastes, ACI Mater. J. 98 (2001) 251–255.
[11] L.E. Copeland, J.C. Hayes, Determination of non-evaporable water in Portland cement pastes, ASTM Bull. 194 (1953) 70–74.
[12] S. Mindess, J.F. Young, Concrete, Prentice-Hall, Englewood Cliffs, NJ, 1981, p. 103.
[13] S. Brunauer, P.H. Emmett, E. Teller, Adsorption of gases in multimolecular layers, J. Am. Chem. Soc. 62 (1940) 723.
[14] E.P. Barrett, L.G. Joyner, P.P. Hallenda, The determination of pore volume and area distributions in porous substances: I. Computations from nitrogen isotherms, J. Am. Chem. Soc. 73 (1951) 373–381.
[15] ASTM C 596-96, Standard test method for drying shrinkage of mortar containing hydraulic cement, Annual Book of ASTM Standards 04.01 (cement; lime; gypsum), American Society for Testing and Materials, West Comshohocken, PA, 2000.
[16] A. Bentur, Effect of curing temperature on the pore structure of tricalcium silicate pastes, J. Colloid Interface Sci. 74 (2) (1980) 549–560.
[17] L.J. Parrott, Effect of a heat cycle during moist curing upon the deformation of hardened cement paste, Hydraulic Cement Pastes, Cem. Concr. Assoc., Slough, UK, 1976, pp. 189–204.
[18] L.J. Parrott, Recoverable and irrecoverable deformation of heat-cured cement paste, Mag. Concr. Res. 29 (98) (1977) 26–30.
[19] L.J. Parrott, Basic creep, drying creep and shrinkage of a mature cement paste after a heat cycle, Cem. Concr. Res. 7 (1977) 597–604.
[20] T. Bergstrom, An environmental scanning electron microscope investigation of drying cement paste: drying shrinkage, image analysis, and modeling, PhD dissertation, Northwestern University, 1993.
[21] A. Bentur, N.B. Milestone, J.F. Young, S. Mindess, Creep and drying shrinkage of calcium silicate pastes: IV. Effect of accelerated curing, Cem. Concr. Res. 9 (2) (1979) 161–170.
[22] B. Tremper, D.L. Spellman, Shrinkage of concrete — comparison of laboratory and field performance, Highway Res. Rec. 3 (1963) 30–61.
[23] G.M. Bruere, J.D. Newbegin, Some aspects of the drying shrinkage of concrete containing chemical admixtures, Proceedings, International Symposium on Admixtures for Mortar and Concrete, vol V.IV, Rilem, Paris, 1967, pp. 61–69.
[24] B.B. Hope, D.G. Manning, Creep of concrete influenced by accelerators, J. Am. Concr. Inst. 68 (1971) 361–365.
[25] R.L. Berger, J.H. Kung, J.F. Young, Influence of calcium chloride on the drying shrinkage of alite pastes, J. Test Eval. 4 (1) (1976) 85–93.
[26] I. Jawed, J. Skalny, Alkalis in cement: a review, Cem. Concr. Res. 8 (1978) 37–51.
[27] G. Pickett, Shrinkage stresses in concrete, Part II, Proc. Am. Concr. Inst. 42 (1946) 361–398.
[28] T.C. Powers, Some aspects of the hydration of Portland cement, J. Port. Cem. Assoc. Res. Dev. Lab. 3 (1961) 47–56.
[29] S. Diamond, Cement paste microstructure — an overview at several levels, Hydraulic Cement Pastes, Cem. Concr. Assoc., Slough, UK, 1976, pp. 2–31.
[30] H.M. Jennings, B.J. Dagleish, P.L. Pratt, Morphological development of hydrating tricalcium silicate as examined by electron microscopy techniques, J. Am. Ceram. Soc. 64 (1981) 567–572.
[31] S. Diamond, D. Bonen, Microstructure of hardened cement paste — a new interpretation, J. Am. Ceram. Soc. 76 (1993) 2993–2999.
[32] H.M. Jennings, P.D. Tennis, Model for the developing microstructure in Portland cement pastes, J. Am. Ceram. Soc. 77 (12) (1994) 3161–3172.
[33] H.M. Jennings, P.D. Tennis, Correction to A model for the developing microstructure in Portland cement pastes, ASTM Bull. 194 (1995) 70–74.
[34] H.M. Jennings, A model for the microstructure of calcium silicate hydrate in cement paste, Cem. Concr. Res. 30 (2000) 101–116.
[35] P.D. Tennis, H.M. Jennings, A model for two types of C–S–H in the microstructure of Portland cement paste, Cem. Concr. Res. 30 (2000) 855–863.
[36] M.C. Garci, H.M. Jennings, Using nitrogen sorption to quantitatively study the microstructure of cement pastes, in: H. Russell (Ed.), High-Performance Concrete: Research to Practice, S.P. 189, American Concrete Institute, Farmington Hills, MI, 1999, pp. 133–145.
[37] C.J. Brinker, G.W. Scherer, Sol–Gel Science, Academic Press, CA, 1990.
[38] C.M. Neubauer, H.M. Jennings, The use of digital images to determine deformation throughout a microstructure: Part II. Application to cement paste, J. Mater. Sci. 35 (2000) 5751–5765.